Robust Control for Linear Induction Motor Servo Drive Using Neural Network Uncertainty Observer

Faa-Jeng Lin†, Rong-Jong Wai‡, Chin-Chung Lee†, and Shu-Peng Hsu†
† Department of Electrical Engineering Chung Yuan Christian University, Chung Li 320, Taiwan
‡ Department of Electrical Engineering Yuan Ze University, Chung Li 320, Taiwan
Phone:886-3-4563171 Ext4814 Fax:886-3-4563160
E-mail: linfj@dec.ee.cycu.edu.tw

Abstract: A robust controller, which combines the merits of integral-proportional (IP) position control and neural network (NN) control, is designed for a linear induction motor (LIM) servo drive in this study. First, the secondary flux of the LIM is estimated using a sliding-mode flux observer on the stationary reference frame and the feedback linearization theory is used to decouple the thrust force and the flux amplitude of the LIM. Then, the IP position controller is designed according to the estimated mover parameters to match the time-domain command tracking specifications. Moreover, a robust controller is formulated using the NN uncertainty observer, which is implemented to estimate the lumped uncertainty of the controlled plant, as an inner-loop force controller to increase the robustness of the LIM servo drive system. Furthermore, in the derivation of the on-line training algorithm of the NN, an error function is used in the Lyapunov function to avoid the real-time identification of the system Jacobian.

1. INTRODUCTION

The LIM has many excellent performance features such as high-starting thrust force, alleviation of gear between motor and the motion devices, reduction of mechanical losses and the size of motion devices, high-speed operation, silence, and so on [1, 2]. Due to the advantages motioned above, the LIM has been used widely in the field of industrial processes and transportation applications [3], e.g., precision positioning in material handling system [3]. The driving principles of the LIM are similar to the traditional rotary induction motor (RIM), but its control characteristics are more complicated than the RIM, and the motor parameters are time-varying due to the change of operating conditions, such as speed of mover, temperature and configuration of rail. Therefore, its mathematical model is difficult to derive completely. Much research has been done for the modelling the dynamic performance of the LIM and taken all the significant variations into consideration [1-3], however, there still exist uncertainties, which usually composed of unpredictable plant parameter variations, external load disturbance, unmodelled and nonlinear dynamics, in practical applications of the LIM. The motivation of this study is to simplify the dynamic model of the LIM and to design a suitable control scheme to confront the existed uncertainties. On the other hand, the dynamic model of the LIM can be modified from the dynamic model of the RIM at certain low speed since the LIM can be visualized to unroll a rotary induction motor. Thus, many decoupled control techniques in RIM can be adopted to decouple the dynamics of the thrust force and the flux amplitude of the LIM. In this study, the nonlinear state feedback theory [4-6] is implemented to decouple the dynamics of the thrust force and the flux amplitude of the LIM. Since accurate flux knowledge is required for the input-output linearization technique, a sliding-mode flux observer [7] is proposed to overcome the mentioned disadvantage of the nonlinear state feedback control. The sliding mode observers have the same robust features as the sliding-mode controllers, such as insensitivity to parameter variations, external disturbance rejection, and fast dynamic response.

With the input-output linearization approach and sliding-mode flux observer, the decoupled control of the LIM is guaranteed. However, the control performance of the LIM is still influenced by the uncertainties of the plant. To deal with the uncertainties, much research has been done in recent years to apply the neural networks in the control field [8-10]. In this study, an NN uncertainty observer is developed to estimate the lumped uncertainty of the motor drive system. Moreover, a robust controller, which combines an IP position controller [11] and the NN uncertainty observer, is proposed to increase the robustness of the LIM servo drive system. In the robust controller, the motor drive system at the nominal condition is selected as the reference model, and the mover position and speed errors between the reference model and the LIM servo drive system are used to estimate the lumped uncertainty based on the NN uncertainty observer.

2. NONLINEAR DECOUPLED CONTROL

The dynamic model of the LIM is modified from the traditional model of a three-phase, Y-connected induction motor in d-q stationary reference frame and can be described by the following differential equations [2]:

$$i_{qs} = -\left(\frac{R_s}{\sigma L_s} + \frac{1-\sigma}{\sigma T_r}\right) i_{qs} - \frac{L_m \pi}{\sigma L_s L_r \tau} v \lambda_{dr} + \frac{L_m}{\sigma L_s L_r T_r} \lambda_{qr} + \frac{1}{\sigma L_s} V_{qs} \quad (1)$$

$$i_{ds} = -\left(\frac{R_s}{\sigma L_s} + \frac{1-\sigma}{\sigma T_r}\right) i_{ds} + \frac{L_m}{\sigma L_s L_r T_r} \lambda_{dr} + \frac{L_m \pi}{\sigma L_s L_r \tau} v \lambda_{qr} + \frac{1}{\sigma L_s} V_{ds} \quad (2)$$

$$\dot{\lambda}_{qr} = \frac{L_m}{T_r} i_{qs} + n_p \frac{\pi}{\tau} v \lambda_{dr} - \frac{1}{T_r} \lambda_{qr} \tag{3}$$

$$\dot{\lambda}_{dr} = \frac{L_m}{T_r} i_{ds} - \frac{1}{T_r} \lambda_{dr} - n_p \frac{\pi}{\tau} v \lambda_{qr} \tag{4}$$

$$F_e = K_f \left(\lambda_{dr} i_{qs} - \lambda_{qr} i_{ds} \right) = M\dot{v} + Dv + F_L \tag{5}$$

where $T_r = L_r / R_r$, $\sigma = 1 - \left(L_m^2 / L_s L_m \right)$, $K_f = 3/2\, n_p (\pi Lm / \tau L_r)$

and

R_s = winding resistance per phase;
R_r = secondary resistance per phase referred primary;
L_m = magnetizing inductance per phase;
L_r = secondary inductance per phase;
L_s = primary inductance per phase;
v = mover linear velocity;
$\lambda_{dr}, \lambda_{qr}$ = d-axis and q-axis secondary flux;
i_{ds}, i_{qs} = d-axis and q-axis primary current;
V_{ds}, V_{qs} = d-axis and q-axis primary voltage;
T_r = secondary time-constant;
σ = leakage coefficient;
F_e = electromagnetic force;
K_f = force constant;
F_L = load disturbance;
M = total mass of the moving element;
D = viscous friction and iron-loss coefficient;
τ = pole pitch;
n_p = number of pole pairs.

2.1. *Feedback Linearization Controller*

The secondary flux amplitude is defined as follows:

$$\lambda_r = \sqrt{(\lambda_{dr})^2 + (\lambda_{qr})^2} \tag{6}$$

and using (3) and (4), the time derivative of λ_r can be derived as follows:

$$\dot{\lambda}_r = -\frac{\lambda_r}{T_r} + \frac{L_m \left(i_{ds} \lambda_{dr} + i_{qs} \lambda_{qr} \right)}{T_r \lambda_r} \tag{7}$$

From (5), the LIM motion dynamics can be expressed as

$$\dot{v} = -\frac{D}{M} v + \frac{K_f}{M} \left(\lambda_{dr} i_{qs} - \lambda_{qr} i_{ds} \right) - \frac{F_L}{M} \tag{8}$$

In the LIM dynamics described by (7) and (8), i_{ds} and i_{qs} are the control inputs, and λ_r and v are the system outputs. Thus, the LIM dynamic is a coupled system. Since there are no direct relations between the outputs and inputs, it is difficult to design the control inputs i_{ds} and i_{qs} so that the system outputs λ_r and v can track the desired trajectories accurately. Therefore, the nonlinear state feedback theory [4-6] is used to eliminate this coupling relationship between the control inputs i_{ds}, i_{qs}, and the system outputs λ_r, v, to simplify the design of the position controller. Two new control inputs u_ϕ and u_T are chosen as follows:

$$\begin{bmatrix} u_\phi \\ u_T \end{bmatrix} = \frac{1}{\lambda_r} \begin{bmatrix} \lambda_{dr} & \lambda_{qr} \\ -\lambda_r \lambda_{qr} & \lambda_r \lambda_{dr} \end{bmatrix} \begin{bmatrix} i_{ds} \\ i_{qs} \end{bmatrix} \tag{9}$$

From (9), the feedback linearization controller can be derived as follows:

$$\begin{bmatrix} i_{ds} \\ i_{qs} \end{bmatrix} = \frac{1}{\lambda_r^2} \begin{bmatrix} \lambda_r \lambda_{dr} & -\lambda_{qr} \\ \lambda_r \lambda_{qr} & \lambda_{dr} \end{bmatrix} \begin{bmatrix} u_\phi \\ u_T \end{bmatrix} \tag{10}$$

Substituting (10) into (7) and (8), the decoupled equations can be obtained as follows:

$$\dot{\lambda}_r = -\frac{\lambda_r}{T_r} + \frac{L_m u_\phi}{T_r} \tag{11}$$

$$\dot{v} = -\frac{D}{M} v + \frac{K_f}{M} u_T - \frac{F_L}{M} \tag{12}$$

Thus, the new inputs u_ϕ and u_T can be used to control the secondary flux amplitude and mover position, respectively. The measurement units of u_ϕ and u_T are ampere (A) and weber•ampere (WbA). However, the secondary flux of the LIM is required to decouple the secondary flux dynamics from the motion dynamics completely. In this study, a sliding-mode flux observer is proposed to estimate the secondary flux.

2.2. *Sliding-Mode Flux Observer*

Rewrite (1)~(4) into the following two parts with $n_p = 1$:

$$\begin{aligned} \frac{d}{dt} \begin{bmatrix} i_{qs} \\ i_{ds} \end{bmatrix} = & \begin{bmatrix} -\left(\frac{R_s}{\sigma L_s} + \frac{1-\sigma}{\sigma T_r} \right) & 0 \\ 0 & -\left(\frac{R_s}{\sigma L_s} + \frac{1-\sigma}{\sigma T_r} \right) \end{bmatrix} \begin{bmatrix} i_{qs} \\ i_{ds} \end{bmatrix} \\ & + \frac{1}{\sigma L_s} \begin{bmatrix} V_{qs} \\ V_{ds} \end{bmatrix} + \begin{bmatrix} \frac{L_m}{\sigma L_s L_r T_r} & -\frac{L_m \pi}{\sigma L_s L_r \tau} v \\ \frac{L_m \pi}{\sigma L_s L_r \tau} v & \frac{L_m}{\sigma L_s L_r T_r} \end{bmatrix} \begin{bmatrix} \lambda_{qr} \\ \lambda_{dr} \end{bmatrix} \end{aligned} \tag{13}$$

$$\frac{d}{dt} \begin{bmatrix} \lambda_{qr} \\ \lambda_{dr} \end{bmatrix} = \begin{bmatrix} \frac{L_m}{T_r} & 0 \\ 0 & \frac{L_m}{T_r} \end{bmatrix} \begin{bmatrix} i_{qs} \\ i_{ds} \end{bmatrix} + \begin{bmatrix} -\frac{1}{T_r} & \frac{\pi}{\tau} v \\ -\frac{\pi}{\tau} v & -\frac{1}{T_r} \end{bmatrix} \begin{bmatrix} \lambda_{qr} \\ \lambda_{dr} \end{bmatrix} \tag{14}$$

Now let

$$\begin{bmatrix} \frac{L_m}{\sigma L_s L_r T_r} & -\frac{L_m \pi}{\sigma L_s L_r \tau} v \\ \frac{L_m \pi}{\sigma L_s L_r \tau} v & \frac{L_m}{\sigma L_s L_r T_r} \end{bmatrix} \begin{bmatrix} \lambda_{qr} \\ \lambda_{dr} \end{bmatrix} = K_B \begin{bmatrix} V_q \\ V_d \end{bmatrix} \tag{15}$$

where $K_B = L_m / \sigma L_s L_r$, and define the switching surface S as follows:

$$S(t) = \begin{bmatrix} \hat{i}_{qs} - i_{qs} \\ \hat{i}_{ds} - i_{ds} \end{bmatrix} \equiv e_i = 0 \tag{16}$$

where $\hat{i}_{ds}$ and $\hat{i}_{qs}$ are the estimated values of i_{ds} and i_{qs}. The sliding-mode current observer is proposed as follows:

$$\frac{d}{dt}\begin{bmatrix}\hat{i}_{qs}\\ \hat{i}_{ds}\end{bmatrix}=\begin{bmatrix}-\left(\frac{R_s}{\sigma L_s}+\frac{1-\sigma}{\sigma T_r}\right) & 0\\ 0 & -\left(\frac{R_s}{\sigma L_s}+\frac{1-\sigma}{\sigma T_r}\right)\end{bmatrix}\begin{bmatrix}\hat{i}_{qs}\\ \hat{i}_{ds}\end{bmatrix} \quad (17)$$
$$+\frac{1}{\sigma L_s}\begin{bmatrix}V_{qs}\\ V_{ds}\end{bmatrix}+K_B\begin{bmatrix}\hat{V}_q\\ \hat{V}_d\end{bmatrix}+K\begin{bmatrix}sgn(\hat{i}_{qs}-i_{qs})\\ sgn(\hat{i}_{ds}-i_{ds})\end{bmatrix}$$

where $\hat{V}_d$ and $\hat{V}_q$ is the estimated value of V_d and V_q; K is the switching gain; sgn$(\cdot)$ is the sign function. Moreover, the secondary flux observer is proposed as follows:

$$\frac{d}{dt}\begin{bmatrix}\hat{\lambda}_{qr}\\ \hat{\lambda}_{dr}\end{bmatrix}=\begin{bmatrix}\frac{L_m}{T_r} & 0\\ 0 & \frac{L_m}{T_r}\end{bmatrix}\begin{bmatrix}\hat{i}_{qs}\\ \hat{i}_{ds}\end{bmatrix}-\begin{bmatrix}\hat{V}_q\\ \hat{V}_d\end{bmatrix} \quad (18)$$

where $\hat{\lambda}_{dr}$ and $\hat{\lambda}_{qr}$ are the estimated values of λ_{dr} and λ_{qr}. Subtracting (13) from (17), the following error dynamic can be obtained:

$$\dot{e}_l = Ae_l + K_B\left[\hat{V}_q - V_q, \hat{V}_d - V_d\right]^T + K\left[\text{sgn}(\hat{i}_{qs}-i_{qs}), \text{sgn}(\hat{i}_{ds}-i_{ds})\right]^T \quad (19)$$

where

$$A=\begin{bmatrix}-\left(\frac{R_s}{\sigma L_s}+\frac{1-\sigma}{\sigma T_r}\right) & 0\\ 0 & -\left(\frac{R_s}{\sigma L_s}+\frac{1-\sigma}{\sigma T_r}\right)\end{bmatrix}$$

If, the switching gain is designed as follows:

$$K=\min\left\{\left(\frac{R_s}{\sigma L_s}+\frac{1-\sigma}{\sigma T_r}\right)|\hat{i}_{qs}-i_{qs}|-K_B\left(\hat{V}_q-V_q\right)\text{sgn}\left(\hat{i}_{qs}-i_{qs}\right)\right. \quad (20)$$
$$\left.\left(\frac{R_s}{\sigma L_s}+\frac{1-\sigma}{\sigma T_r}\right)|\hat{i}_{ds}-i_{ds}|-K_B\left(\hat{V}_d-V_d\right)\text{sgn}\left(\hat{i}_{ds}-i_{ds}\right)\right\}-\delta$$

where δ is a positive small value, the globally asymptotical stability of (19) can be guaranteed. The proof is omitted here.

Since the sliding-mode condition is satisfied with a sufficient small switching gain K, then

$$\dot{e}_l = e_l = 0 \quad (21)$$

Using (19) and (21), a switching function K_a can be defined as follows:

$$K_a = K_B\left[\hat{V}_q - V_q, \hat{V}_d - V_d\right]^T = -K\left[\text{sgn}(\hat{i}_{qs}-i_{qs}), \text{sgn}(\hat{i}_{ds}-i_{ds})\right]^T \quad (22)$$

According to (22), $\hat{V}_q$ and $\hat{V}_d$ can be obtained by the following equation:

$$\begin{bmatrix}\hat{V}_q\\ \hat{V}_d\end{bmatrix}=\begin{bmatrix}V_q\\ V_d\end{bmatrix}-\frac{K}{K_B}\begin{bmatrix}\text{sgn}(\hat{i}_{qs}-i_{qs})\\ \text{sgn}(\hat{i}_{ds}-i_{ds})\end{bmatrix} \quad (23)$$

Then the estimated secondary flux $\hat{\lambda}_{qr}$ and $\hat{\lambda}_{dr}$ can be obtained using (18).

A block diagram of the nonlinear decoupled LIM servo drive system combined with a sliding-mode flux observer is shown in Fig. 1, which consists of a ramp-comparison current-controlled pulse width modulated (PWM) voltage source inverter (VSI), a feedback linearization controller, two coordinate translators, a speed-control loop, and a position control loop. By use of the nonlinear decoupled technique, the LIM servo drive shown in Fig. 1 can be reasonably represented by the control system block diagram shown in Fig. 2, in which

$$F_e = K_f u_T \quad (24)$$

$$H_p(s) = \frac{1}{Ms+D} = \frac{b}{s+a} \quad (25)$$

where u_T is the thrust current command, and s is the Laplace operator. To match the requirements of motor drive applications, the desired specifications of position step command tracking usually are: (i) no overshoot; (ii) no steady-state error; (iii) preset of rise time, t_{re}. A systematic design procedure for an integral-proportional (IP) position controller capable of satisfying the above specifications has been introduced by Lin [11]. The closed-loop drive system with an IP position controller is shown in Fig. 2. Though the desired command tracking response can be obtained using an IP position controller in the nominal case, the performance of the IP control system is sensitive to parameter variations and external disturbances in the plant. To solve this problem, a robust controller combining an IP position controller and an NN uncertainty observer is proposed in the following section.

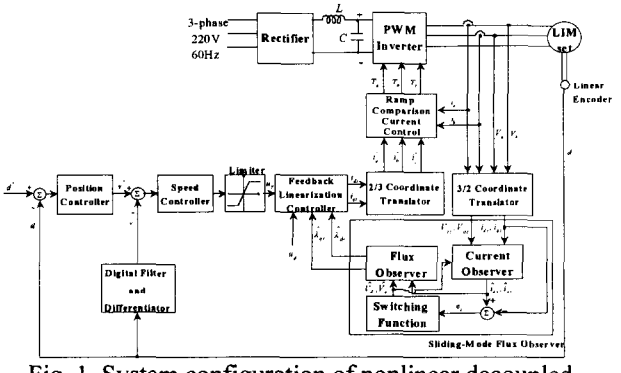

Fig. 1. System configuration of nonlinear decoupled LIM servo drive.

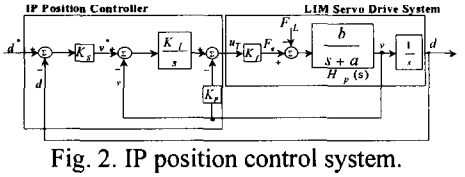

Fig. 2. IP position control system.

3. ROBUST CONTROLLER WITH NN UNCERTAINTY OBSERVER

In the robust controller, the proposed NN uncertainty observer is augmented to the IP control system to preserve the desired command tracking response under the occurrence of uncertainties. A block diagram of the robust control system is shown in Fig. 3, in which the IP position controller is the main tracking controller, and the NN

uncertainty observer is designed to compensate the degenerate response under the occurrence of uncertainties.

3.1. Robust Controller

Consider the motor drive system, as shown in Fig. 3, in the nominal condition without external load disturbance, the following equations can be obtained from (12):

$$\dot{v} = -\frac{\overline{D}}{\overline{M}}v + \frac{K_f}{\overline{M}}u_T \tag{26}$$

where the "—" symbol represents the system parameters in the nominal condition. The above equation is the dynamic of the nominal LIM servo drive system, which is selected as the reference model. Equation (26) can be formulated into the following state-space form:

$$\dot{X}_m = A_m X_m + B_m U_m \tag{27}$$

where

$$X_m = v_m,\quad A_m = -\overline{D}/\overline{M},\quad B_m = K_f/\overline{M}$$

and U_m denotes the input of the reference model; v_m denotes the output of the reference model. Now, consider (29) with parameter variations and external load disturbance for the actual LIM servo drive system, then

$$\dot{X}_P = (A_m + \Delta A)X_p + (B_m + \Delta B)U_P + CF_L \tag{28}$$

where $X_P = v$; $C = -1/M$; ΔA and ΔB denote the uncertainties introduced by system parameters M and D; U_P is the control input to the motor drive system, i.e., u_T. Reformulate (29), then

$$\dot{X}_p = A_m X_p + B_m(U_P + E) \tag{29}$$

where E is named the lumped uncertainty and defined by

$$E \triangleq B_m^+(\Delta A X_P + \Delta B U_P + CF_L) \tag{30}$$

where B_m^+ is the left penrose pseudo inverse of B_m, i.e., $B_m^+ = (B_m^T B_m)^{-1} B_m^T$.

The lumped uncertainty E is assumed to be a constant during the observation. The above assumption is valid in practical digital processing of the observer because the sampling period of the observer is short enough compared with the variation of E. Let e and $\dot{e}$ denote the mover position error and the mover speed error between the reference model and actual LIM servo drive system, i.e.,

$$e \triangleq d_m - d \tag{31}$$

$$\dot{e} \triangleq v_m - v \tag{32}$$

where d_m and d are the desired and actual mover position, respectively. Then an error function is defined as follows:

$$S_e = \dot{e} + \lambda e \tag{33}$$

where λ is a positive scalar. Since the lumped uncertainty E is unknown in actual application, an NN uncertainty observer is proposed in the next section to observe the value of the lumped uncertainty. The robust control law is defined as follows:

$$U_P = U_m - \hat{E} + B_m^+(\lambda\dot{e} - A_m\lambda e) \tag{34}$$

where $\hat{E}$ is the observed value of the lumped uncertainty and the measurement unit is WbA. Moreover, the error between the observed and actual values of the lumped uncertainty can be presented by

$$\tilde{E} = \hat{E} - E \tag{35}$$

From (27), (29), (32), (33) and (34), the error dynamic of the robust control system is

$$\dot{S}_e = A_m S_e + B_m \tilde{E} \tag{36}$$

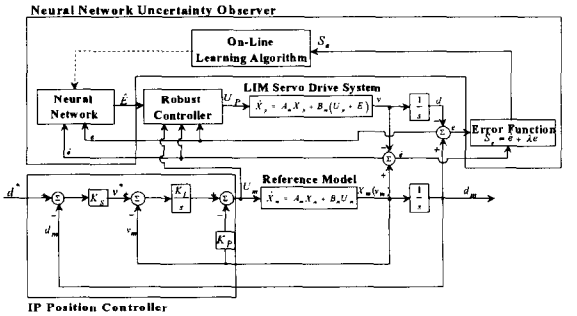

Fig. 3. Robust control system.

3.2. Neural Network Uncertainty Observer

A three-layer neural network [8-10], as shown in Fig. 4, which comprises an input (the i layer), a hidden (the j layer) and an output layer (the k layer), is adopted to implement the proposed NN uncertainty observer. The inputs of the NN uncertainty observer are e and $\dot{e}$; the output of the NN is the observed value of the lumped uncertainty $\hat{E}$. The connective weights and biases of the NN are adjusted on line to produced $\hat{E}$. Moreover, using the proposed robust controller the error between the state of the reference model and the LIM servo drive system will make a continuous updating of $\hat{E}$ to steer the state of the drive system to follow the state of the reference model. The signal propagation and the basic function in each layer are introduced below.

Input Layer

$$net_i = x_i, O_i = f_i(net_i) = net_i, i = 1,2 \tag{37}$$

where $x_1 = e(t)$ and $x_2 = \dot{e}(t)$.

Hidden Layer:

$$net_j = \sum_i (W_{ji} O_i) + \theta_j$$

$$O_j = f_j(net_j) = \frac{1}{1 + e^{-net_j}}, j = 1, \cdots, m \tag{38}$$

where W_{ji} are the connective weights between the input and the hidden layers; θ_j are the threshold values for the units in the hidden layer; f_j is the activation function, which is a sigmoidal function.

Output Layer:

$$net_k = \sum_j (W_{kj} O_j), O_k = f_k(net_k) = net_k, k = 1 \tag{39}$$

where W_{kj} are the connective weights between the hidden and the output layers; $O_k = E$.

In the proposed on-line learning algorithm of the NN, the Lyapunov function V_e is defined as $V_e = 0.5S_e^2$. The choice of S_e in the Lyapunov function has the merit that

the Jacobian of the controlled plant is not needed in the on-line learning algorithm.

Multiplying (36) both sides by S_e, the following equation can be obtained:

$$S_e\dot{S}_e = A_m S_e^2 + B_m \tilde{E} S_e \tag{40}$$

According to the gradient descent method, the weights in the output layer are updated by the following equation:

$$\dot{W}_{kj} = -\frac{\partial S_e \dot{S}_e}{\partial \hat{E}} \frac{\partial \hat{E}}{\partial O_k} \frac{\partial O_k}{\partial net_k} \frac{\partial net_k}{\partial W_{kj}} = -B_m S_e O_j \tag{41}$$

Moreover, the approximated error term needs to be calculated and propagated by the following equation:

$$\delta_k = -\frac{\partial S_e \dot{S}_e}{\partial net_k} = -B_m S_e \tag{42}$$

The weights in the hidden layer are updated by the following equation:

$$\dot{W}_{ji} = -\frac{\partial S_e \dot{S}_e}{\partial net_k} \frac{\partial net_k}{\partial O_j} \frac{\partial O_j}{\partial net_j} \frac{\partial net_j}{\partial W_{ji}} = \delta_k W_{kj} f'(net_j) O_i \tag{43}$$

The bias of each neuron in the hidden layer is also trained using the same algorithm. Since the gradient vector is calculated in the direction opposite to the energy flow, the convergence properties of the NN can depend on the nature convergence characteristics of the gradient search algorithm [8-10]. The proposed NN uncertainty observer can guarantee the tracking error to be zero. However, the guaranteed convergence of tracking error to be zero does not imply convergence of the observed value of the lumped uncertainty to the real value.

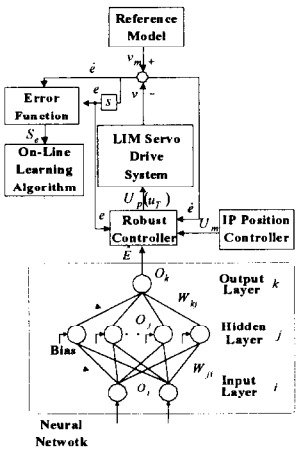

Fig. 4. Block diagram of NN uncertainty observer.

4. Experimental Results

The LIM used in this drive system is a three-phase Y-connected two-pole 3kW 60Hz 180V/14.2A type. The detailed parameters of the LIM are

$$u_\phi = 2\text{A},\ R_s = 5.369\Omega,\ R_r = 3.532\,\Omega,\ \tau = 0.027\text{m}$$
$$L_m = 0.024\text{H},\ L_s = 0.028\text{H},\ L_r = 0.028\text{H} \tag{44}$$

where u_ϕ is the flux current command. Moreover, the curve fitting technique based on step response is applied to find the drive model off line at the nominal case ($F_L = 0$). The results are (on a scale of 1.5915 (m/s)/V)

$$K_f = 148.35\text{N/WbA} \quad a = 12.965 \quad b = 0.226$$
$$\overline{M} = 2.78\text{kg} \triangleq 4.425\text{Ns/V}$$
$$\overline{D} = 36.0455\text{kg/s} \triangleq 57.366\,\text{N/V} \tag{45}$$

A co-processor computer control system is designed for the LIM servo drive. The feedback linearization controller, the IP position controller and the robust controller with NN uncertainty observer are realized in a Pentium CPU, moreover, the sliding-mode flux observation system is realized in a TMS320C32 DSP. The control intervals of the feedback linearization controller and the observation system are set at 0.2msec, and the control interval of the position control loop is set at 1msec. The control objective is to control the mover to move 0.1m periodically.

To investigate the effectiveness of the proposed feedback linearization controller and sliding-mode flux observer, the nominal design gains of the IP position controller shown in Fig. 2 for a rise-time setting at 0.4sec are as follows [11]:

$$K_S = 5.05, K_P = 20.212, K_I = 429.053 \tag{46}$$

In addition, the parameters in (20) and (25) are given as follows:

$$\delta = 0.1,\ \gamma_o = 1,\ \varepsilon = 0.01 \tag{47}$$

These parameters shown in (47) are chosen to achieve the best transient control performance in both the simulation and experimentation considering the requirement of asympotical stability and the possible operating conditions.

Some experimental results are provided to demonstrate the effectiveness of the proposed nonlinear decoupled control scheme. A low-pass filter is used to smooth the estimated secondary flux. The responses of the nonlinear decoupled control scheme due to step-command change 0.1m are shown in Fig. 5. The position response of the mover is shown in Fig. 5(a); the observed values of *d*-axis and *q*-axis secondary fluxes are shown in Figs. 5(b) and 5(c); the associated three-phase command and actual currents are shown in Figs. 5(d), 5(e) and 5(f). Good decoupled control performance yielded by the proposed feedback linearization controller and the sliding-mode flux observer is obvious from the experimental results.

Some experimental results are provided to demonstrate the effectiveness of the proposed robust controller. Two test conditions are provided, which are the nominal case and the parameter variation case. In the experimentation, the parameter variation case is the addition of one iron disk with 8.34kg weight to the mass of the mover. The experimental results of the IP position controller at the nominal case and parameter variation case for a periodic step command are shown in Fig. 6. The position responses of the mover are shown in Figs. 6(a) and 6(c); the associated control efforts are shown in Figs. 6(b) and 6(d). From the experimental results, poor tracking responses are resulted for the position of mover under the condition of parameter variation. Moreover, the experimental results of the robust controller at the nominal case and parameter variation case for a periodic step command are shown in

Fig. 7. The position responses of the mover are shown in Figs. 7(a) and 7(d); the associated control efforts are shown in Figs. 7(b) and 7(e); the observed lumped uncertainties are shown in Figs. 7(c) and 7(f). The observed lumped uncertainty shown in Fig. 7(c) is resulted owing to the unmodelled dynamics in practical applications, which are regarded as the uncertainties and observed by the NN uncertainty observer. From the experimental results, the degenerate position response is much improved under the occurrence of parameter variation with the nominal drive model as the reference model in the robust control system.

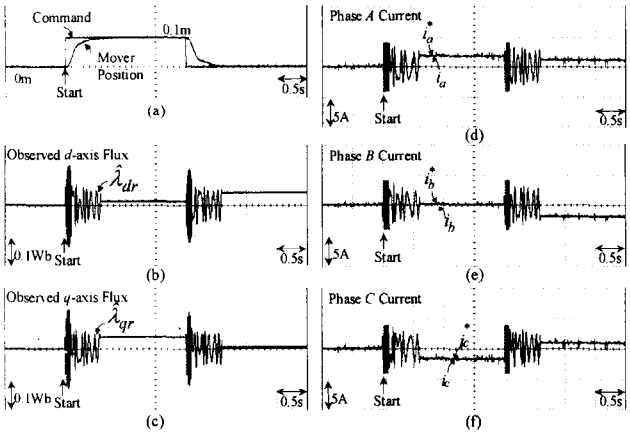

Fig. 5. Experimental results of decoupled control.

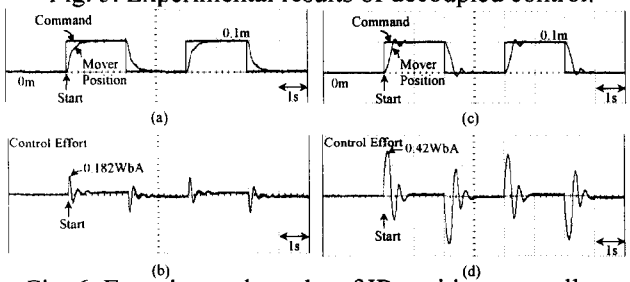

Fig. 6. Experimental results of IP position controller.

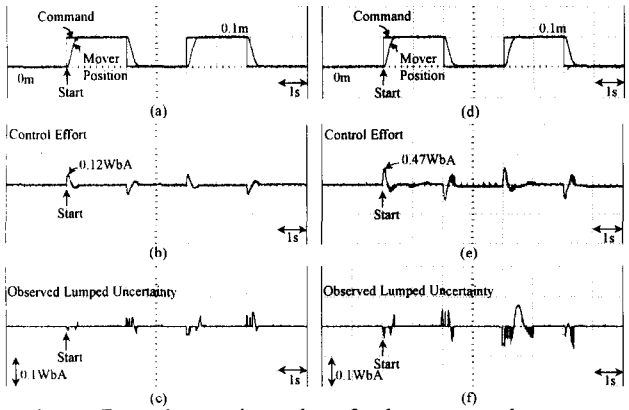

Fig. 7. Experimental results of robust control system.

5. CONCLUSIONS

This study has successfully demonstrated the applications of a robust controller, which comprises an IP position controller and the proposed NN uncertainty observer, to the position control of a LIM servo drive. First, the secondary flux of the LIM was estimated with a sliding-mode flux observer, and the feedback linearization controller was used to decouple the thrust force and the flux amplitude of the LIM. Then, a robust controller was formulated using the NN uncertainty observer, which was implemented to estimate the lumped uncertainty of the controlled plant, to increase the robustness of the LIM servo drive system. The effectiveness of the proposed control schemes has been confirmed by some experimental results.

ACKNOWLEDGMENTS

The author would like to acknowledge the financial support of Chung Yuan Christian University, Taiwan, R.O.C.

REFERENCES

[1] I. Takahashi, and Y. Ide, "Decoupling control of thrust and attractive force of a LIM using a space vector control inverter," *IEEE Trans. Ind. Appl.*, vol. 29, no. 1, pp. 161-167, 1993.

[2] I. Boldea, and S. A. Nasar, *Linear Electric Actuators and Generators*. Cambridge University Press, 1997.

[3] G. H. Abdou, and S. A. Sherif, "Theoretical and experimental design of LIM in automated manufacturing systems," *IEEE Trans. Ind. Appl.*, vol. 27, no. 2, pp. 286-293, 1991.

[4] G. S. Kim, I. J. Ha, and M. S. Ko, "Control of induction motors for both high dynamic performance and high power efficiency," *IEEE Trans. Ind. Electron.*, vol. 39, no. 4, pp. 323-333, 1992.

[5] R. Marino, S. Peresada, and P. Valigi, "Adaptive input-output linearizing control of induction motors," *IEEE Trans. Automatic Control*, vol. 38, no. 2, pp. 208-221, 1993.

[6] M. Bodson, J. Chiasson, and R. Novotnak, "High-performance induction motor control via input-output linearisation," *IEEE Control Syst. Mag.*, vol.14, no. 4, pp. 25-33, 1994.

[7] F. J. Lin, R. J. Wai, and P. C. Lin, "Robust speed sensorless induction motor drive," *IEEE Trans. Aerospace and Electric Systems*, vol. 35, no. 2, pp. 566-578, 1999.

[8] K. S. Narenda, and K. Parthasarathy, "Identification and control of dynamical systems using neural networks," *IEEE Trans. Neural Networks*, vol. 1, pp. 4-27, 1990.

[9] J. R. Noriega and H. Wang, "A direct adaptive neural-network control for unknown nonlinear systems and its application," *IEEE Trans. Neural Network*, vol. 9, no. 1, pp. 27-34, 1998.

[10] F. J. Lin, W. J. Hwang, and R. J. Wai, "A Supervisory Fuzzy Neural Network Control System for Tracking Periodic Inputs, " *IEEE Trans. Fuzzy Systems*, vol. 7, no. 1, pp. 41-52, 1999.

[11] F. J. Lin, "Real-time IP position controller design with torque feedforward control for PM synchronous motor," *IEEE Trans. Ind. Electron.*, vol. 44, no. 3, pp. 398-407, 1997.